Hindawi
Shock and Vibration
Volume 2022, Article ID 8706397, 11 pages
https://doi.org/10.1155/2022/8706397

Research Article

Variation of Permafrost Upper Limit in Permafrost Subgrade Covered by Snow on Steep Slope of Alpine Mountains

Zhilong Zhang and Xiancheng Li

School of Civil Engineering and Architecture, Xinjiang University, Urumqi 830047, China

Correspondence should be addressed to Xiancheng Li; lxc23456@stu.xju.edu.cn

Received 19 May 2022; Revised 1 June 2022; Accepted 6 June 2022; Published 27 June 2022

Academic Editor: Yonggang Zhang

The thermal insulation effect of snow on the active layer thickness of permafrost cannot be ignored. Under the dual influence of snow cover and roadbed construction, this paper studies the influence of snow cover on the temperature field and permafrost upper limit under the permafrost roadbed in the alpine mountains. Through the application of PDE module in Comsol software, the hydrothermal coupling analysis of roadbed is carried out by means of numerical analysis. The results show that the permafrost degradation is accelerated by the snow on the subgrade surface, the temperature increases significantly, the thickness of the active layer increases, and the permafrost upper limit moves downward. With the increase of seasonal snow thickness, the permafrost temperature under the subgrade increases, the low-temperature permafrost under the subgrade has the risk of changing to high-temperature permafrost. The melting groove is formed under the subgrade on the right side, and with the increase of snow thickness, the area of the melting groove expands and develops towards the center of the subgrade. Permafrost upper limit on the left and right shoulder is lower than that on the right shoulder, and snow cover has a greater impact on permafrost upper limit on the right shoulder.

1. Introduction

At present, more and more road projects are built in the alpine mountains, which are covered by snow for a long time, the space distribution of snow cover is very uneven, and the difference in the vertical zone is very significant. The snow cover is concentrated in the cold mountain areas, especially the Altai Mountains, Tianshan Mountains, Nyainqentanglha Mountains, and Tanggula Mountains, where the snow depth is more than 30 cm to 50 cm [1]. Snow cover in Asia can be divided into perpetual snow cover areas and seasonal snow cover areas (stable and unstable snow cover areas). Among them, the Tianshan Mountains, Karakoram Mountains, Kunlun Mountains, Pamirs, Himalayas, Nyainqentanglha Mountains, Tanggula Mountains, and Bayankala Mountains are all in stable snow cover areas, and their snow depth in winter is greater than 20 cm [2]. The Tianshan Mountains are one of the largest mountain systems in Asia. The Yili River Basin in the Tianshan Mountains has the thickest snow cover, and the snow depth generally exceeds 60 cm. The snow depth of Tianshan Mountain and the maximum snow depth of Ili are as high as 129 cm and 80 cm, respectively. The snow depth of the northern slope of Tianshan Mountain is usually 30 cm to 55 cm [3].

As a substance with high emissivity and low thermoconductivity [4, 5], snow cover causes variations in the heat conditions of its soil underneath [6, 7]. Snow cover results in the warming of perpetual snow cover in north regions and may be even more vital in future Arctic warming scenarios [8, 9]. The snow cover results in the interface for thermal exchange between the surface and the environment moving [10, 11], and the weak thermoconductivity and large heat capacity of snow avoids the loss of surface heat. Melissa et al.; Zhang et al.; Wu [12–14] quantified the influence of the increase of snow cover and the time of snow cumulation on soil heat status. The monthly soil temperature under 54 cm snow cover was 7.7 to 9.9°C higher than that under 10 cm snow cover. The time of snow cover also had a great

influence on soil temperature in winter, and the maximum active layer thickness and snow depth had a significant influence. Haeberli [15] successfully used the association between the bottom temperature of snow layer and surface temperature in the Alps in late winter to map the permafrost distribution in the Alps and other regions with heavy snow. Stieglitz et al. and Park et al. [6, 16] discovered that apart from warming temperatures, snow cover was also vital for the identified warming of arctic permafrost. Poglioti et al.; Han et al. [17, 18] believe that snow cover may only exert a main impact on the interannual variation of active layer thickness in the Alps. This makes the snow have a specific thermoinsulation effect on the Earth's surface. Wang et al. 2012 calculated the data on the snow cover and freezing depth per day in the Altay region of Xinjiang. It is found that when the depth of snow cover is 20 cm to 40 cm, the freezing depth of the frozen soil beneath the snow cover will be reduced by 15 cm to 50 cm. Fu et al.; Pan et al.; Pan et al. [19–21] verified that snow cover could hinder the effect of air temperature on the thickness of frozen soil. The appearance time of maximal freezing depth in the natural snow (NS), compacted snow (CS), and thickened snow (TS) treatments was postponed by 7, 12, and 20 days, separately, in contrast to the bare ground. Zhang et al. studied the effects of seasonal snow cover on ground thermal transfer, soil freezing and thawing, and permafrost developmental process. Yu et al.; Zhong et al. [22, 23] and others conducted long-term investigations on the air and soil temperature in the presence of absence of snow cover. The study discovered that snow cover could remarkably postpone the variation of soil temperature. Li et al. [24] discussed the effect of snow cover on the temperature field of frozen soil roadbed in cold regions by numerical calculation of frozen soil roadbed with and without snow. Snow cover increases the frozen soil's upper limit below the roadbed.

The current studies mainly focus on the change mechanism of the snow cover on the frozen soil's temperature field and upper limit. However, the road construction in the cold mountain areas needs to pass through the frozen soil section with a steeper slope, most of the roadbeds in these sections are part-cut part-fill roadbeds, and studies on this are rare. Given the above characteristics, this manuscript analyzes the temperature field of the roadbed in the cold mountain areas, which is below the snow cover, by numerical calculation. It also studies the changes in the upper limit and temperature of the frozen soil roadbed under the effects of snow cover and road status. This has specific guiding value for infrastructure development in cold mountain regions.

2. Mathematical Model

2.1. Temperature Field Governing Equation. Assuming that the soil is a persistent, uniform, and isotropical medium. According to Fourier's law of thermal conduction and the law of conservation of energy [25], the latent heat of ice-water phase transition is considered as a thermal source, and the control equation of the temperature field of unsaturated soil is shown as follows.

$$\rho C(\theta)\frac{\partial T}{\partial t} = \lambda(\theta)\nabla^2 T + L\rho_I\frac{\partial \theta_I}{\partial t}, \tag{1}$$

where ρ and ρ_I denote the soil and ice densities, respectively, kg/m^3; $C(\theta)$ denotes the specific heat of the soil, J/(kg•°C); θ denotes the volumetric water content in the soil; T denotes the temperature of the soil, °C; t denotes time, s; $\lambda(\theta)$ denotes soil thermoconductivity, W/(m•°C); ∇ denotes differential operator; L denotes latent heat of ice-water phase transition, which is taken as 334.5 kJ•kg^{-1}; and θ_I is the volume fraction of ice. The water θ in the frozen soil comprises pore water θ_u and pore ice. Because the densities of water and ice are different, the volumetric moisture content in the frozen soil is defined as $\theta = \theta_u + \rho_I/\rho_w \cdot \theta_I$.

As shown in the formula, the volumetric heat capacity and thermoconductivity consider the phase transition interval of frozen soil.

$$\begin{cases} C = C_f + H(T)\left(C_u - C_f\right), \\ \lambda = \lambda_f + H(T)\left(\lambda_u - \lambda_f\right). \end{cases} \tag{2}$$

in which f and u denote completely frozen and completely thawed states, separately; C_f and C_u denote the specific heat per unit mass of frozen soil and thawed soil, J/(kg•K); λ_f and λ_u denote the thermoconductivity of frozen soil and thawed soil, separately, W/(m•K); $H(T)$ is a step function.

2.2. Water Field Control Equation. The seepage of unfrozen water in frozen soil is in accordance with Darcy's law. As per the law of conservation of mass, the diversity in water quality between inflow and outflow per unit time is numerically equivalent to the variation in soil water quality. Only the interstitial potential and gravity potential are considered, the governing equation of the water field is shown as follows.

$$\frac{\partial \theta_u}{\partial t} + \frac{\rho_I}{\rho_w}\frac{\partial \theta_I}{\partial t} = \nabla\left(D(\theta_u)\nabla\theta_u + k_g(\theta_u)\right), \tag{3}$$

where θ_u denotes the water content of unfrozen water; ρ_w is the density of liquid water (kg/m^3); $D(\theta_u)$ is the diffusion coefficient of unfrozen water; and $k_g(\theta_u)$ is the permeability coefficient in the direction of gravitational acceleration (m/s).

The diffusivity of water in frozen soil is shown in the following equation.

$$D(\theta_u) = \frac{K(\theta_u)}{C(\theta_u)}. \tag{4}$$

Relative saturation is defined as shown in the following equation.

$$S = \frac{\theta_u - \theta_r}{\theta_s - \theta_r}. \tag{5}$$

The hydraulic conductivity of soil is obtained by the V-G model [26] as shown in the following equation.

$$K(\theta_u) = K_s \cdot S^l \cdot \left(1 - \left(1 - S^{1/m}\right)^m\right)^2. \quad (6)$$

Specific water capacity represents the quantitative relationship between soil water potential and volumetric water content under isothermal conditions.

$$c(\theta_u) = a_0 \cdot \frac{m}{1-m} \cdot S^{1/m} \cdot \left(1 - S^{1/m}\right)^m. \quad (7)$$

Consider the impedance effect of ice on unfrozen water [27].

$$I = 10^{-10 \cdot \theta_I}, \quad (8)$$

where, m, and l are the determined constitutive parameters according to soil properties; K_s denotes the permeation coefficient of saturated soil.

The water field and temperature field equations determined by Equations (1) and (2) contain three unknowns, temperature, pore ice, and unfrozen water content, and the relationship between them can be determined according to the solid-liquid ratio B_I [28].

$$B_I = \frac{\theta_I}{\theta_u} = \begin{cases} 1.1 \cdot \left(\dfrac{T}{T_f}\right)^B - 1.1, & T < T_f, \\ 0, & T \geq T_f. \end{cases} \quad (9)$$

3. Model Validation

3.1. Verification of the Effect of Snow Cover on Ground Insulation. Through the secondary development of PDE module in COMSOL, the above water-thermal coupling equation is expressed in COMSOL, and the following numerical calculation is performed. To verify the thermoinsulation effect of snow cover on the superficial temperature and the accuracy of the selected snow cover parameters, in COMSOL porous media heat transfer module, snow of different thickness is regarded as a layer of material with poor thermal conductivity to cover the subgrade surface, and thermal boundary conditions are added to the surface of snow to simulate the ground temperature under snow cover. The experimental results of Reference [29] were compared with the simulation results. The density variation of snow cover at different depths is ignored in the simulation process. The density of snow is regarded as uniform distribution. After the snowfall, the average density of snow cover is 190 kg/m^3 [30]. The snow thawing time is short, and this process has little effect on the superficial temperature under the snow cover, so that it can be ignored. The snow cover variables are shown in Table 1.

As shown in Figure 1, the maximum error between the experimental value and the calculated value of the surface temperature below the 20 cm snow cover is 0.7°C. The simulated values are basically consistent with the experimental values in Reference [29], which indicates that the snow cover parameters are reasonably selected and the calculation model is reliable.

Table 1: Snow cover model variables.

C J/(kg · K)	λ W/(m · K)	ρ kg/m^3	Porosity
21000	0.29	190	0.72

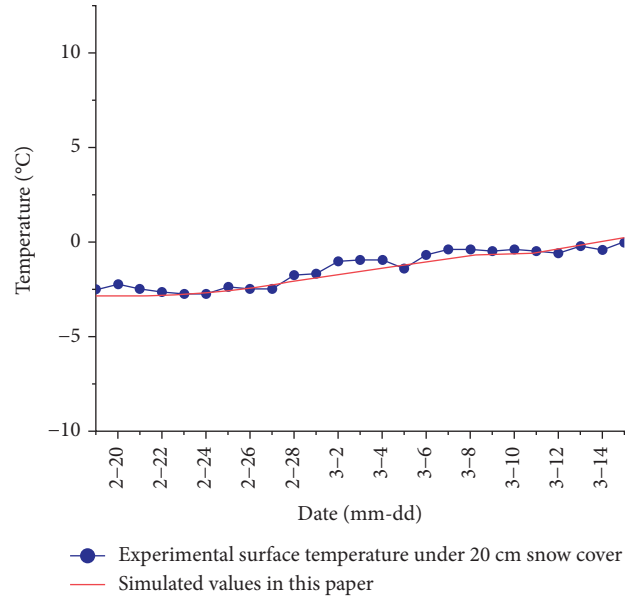

Figure 1: Surface temperature with and without snow cover.

3.2. Mathematical Model Verification. This manuscript verifies the validity and feasibility of the above-mentioned hydrothermal coupling numerical model according to the soil column thawing experiment under closed conditions in the literature [31]. Xu selected Lanzhou silt with an initial moisture content of 22.3% to make a soil column with a height of 10 cm and a diameter of 10 cm. The initial temperature of the soil column was −1°C, and the temperature at the top of the soil column was always kept at 1°C, and the temperature at the bottom was −1°C during the experiment process.

The COMSOL software was used to establish a two-dimensional soil column model, and its length and height were both 10 cm. The temperature and moisture field's initial and boundary conditions are the same as the experiments in Reference [31]. According to Reference [32], Lanzhou silt parameters are displayed in Table 2. The moisture content and temperature distribution obtained from experiments and numerical simulations after thawing for 120 hours are shown in Figures 2 and 3.

It can be seen from Figures 2 and 3 that the simulative outcomes coincide with the experimental values of soil column thawing in Reference [31]. After the soil column is thawed for 120 hours, the freeze-thaw interfacial region is at the height of about 4 cm of the soil column. After the upper part of the soil column is thawed, the soil moisture migrates to the freeze-thaw interface under the combined influence of the interstitial potential and the gravity potential. This results in that the water content of the upper part of the thawed area is significantly lower than the initial moisture content.

Table 2: Model parameters of thawing experiments.

a_0 (m^{-1})	m	θ_s	θ_r	B	K_s (m/s)	T_f (°C)	C_f [J/(kg ·K)]	C_u [J/(kg ·K)]	λ_f [W/(m ·K)]	λ_u [W/(m ·K)]
1.6	0.26	0.42	0.02	0.47	3×10^{-7}	−0.24	1200	1300	1.2	1.0

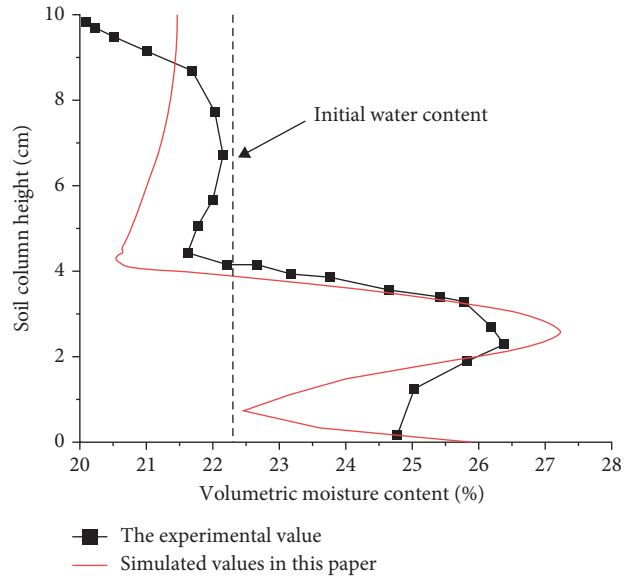

Figure 2: Distribution of volumetric water content in samples.

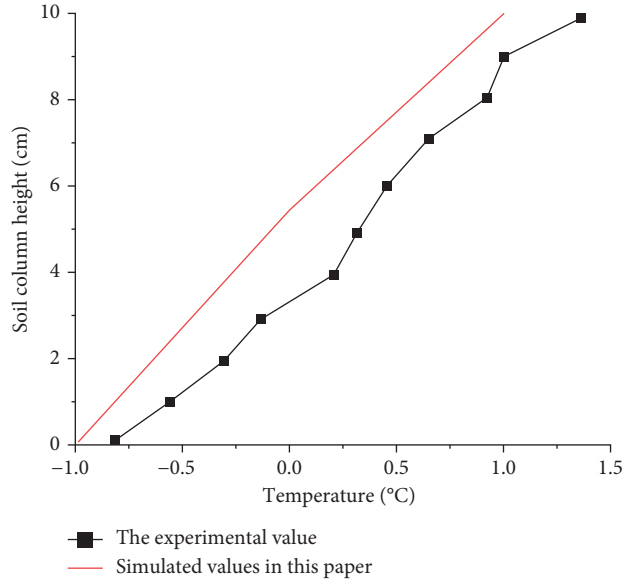

Figure 3: Temperature distribution in samples.

The water content in the lower half of the soil column elevated and then decreased, and the peak moisture content appeared near the freeze-thaw interfacial region. The water from the thawing zone stays near the freeze-thaw interfacial region due to the blocking effect of ice. The peak water content occurred near the freeze-thaw interfacial region. The temperature of the soil column has the same trend as the experimental value, and the temperature value is close. The mathematical model used in this manuscript can more accurately simulate the water migration and temperature field changes in frozen soil. The modified model can analyze the roadbed temperature field in frozen soil regions.

4. Model Establishment

4.1. Geometric Model and Physical Parameters. The width of the upper and lower slopes of the roadbed model is 30 m. The roadbed is 8 m wide, the depth below the roadbed is 50 m, the natural slope is 15°, and the side slope is 1 : 1.5. The model is detailed in Figure 4. Its left and right sides are adiabatic boundaries. Assuming that surface evaporation and precipitation are kept in balance, the surface, the left and right sides of the roadbed, and the bottom of the model are all zero flux boundaries. Zhang et al., the hydrothermal variables of the soil layer are displayed in Table 3.

4.2. Boundary Conditions. The surface temperature and wind speed data, monitored by the unmanned automatic weather station at the Y5854 site (3227 m above sea level) in Bazhou and Jingxian, were selected. The ground temperature from 2014 to 2015 is shown in Figure 5. To distinguish whether the atmospheric heating effect or the snow cover insulation effect affect the frozen soil, the thermal boundary condition does not consider atmospheric warming under the boundary layer's effect [33]. The temperature boundary conditions of the naturally formed ground surface are obtained by fitting, as displayed by Equation (10). The temperature boundary conditions of the roadbed surface and the slope surface are obtained by fitting, as shown in Equations (11) and (12), respectively.

In the cold mountain areas of Xinjiang, the wind speed is high, and the phenomenon of wind blowing snow is serious. The snow cover on the roadbed with large slopes and hillside are thin and accumulated in their deep depressions [34, 35]. As shown in Figure 6, the average ten-minute wind speed is 4.8 m/s when winter snow cover occurs. The maximum wind speed can reach about 25 m/s, and the wind speed can often reach grades 7 to 9. Therefore, only the impact of snow cover on the roadbed superficial area is considered in the calculation process.

The natural slope temperature is

$$T = -2.9 + 12\sin\left(\frac{2\pi t}{8760} - 0.56\pi\right). \quad (10)$$

The roadbed surface temperature is

$$T = -2.4 + 15\sin\left(\frac{2\pi t}{8760} - 0.56\pi\right). \quad (11)$$

The roadbed slope temperature is

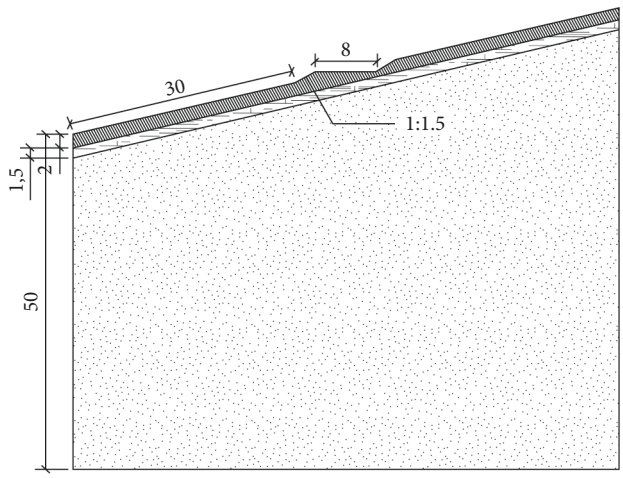

Figure 4: Two-dimensional calculation model of roadbed (unit: m).

Table 3: Main parameters of roadbed model.

Lithology	m	θ_s	θ_r	θ_0	a_0 (m^{-1})	ρ ($kg{\cdot}m^{-3}$)	K_s (m/s)	C_f [J/(kg·K]	C_u [J/(kg ·K]	λ_f [W/(m ·K]	λ_u [W/(m ·K]
Gravel soil	0.26	0.25	0.01	0.08	0.45	2100	4×10^{-6}	870	1060	1.5	1.4
Low clay	0.26	0.4	0.02	0.20	3.28	1920	4×10^{-7}	1140	1270	1.8	1.5
Mudstone	0.26	0.1	0.01	0.90	0.80	2200	2×10^{-9}	1200	1350	2.5	2.0

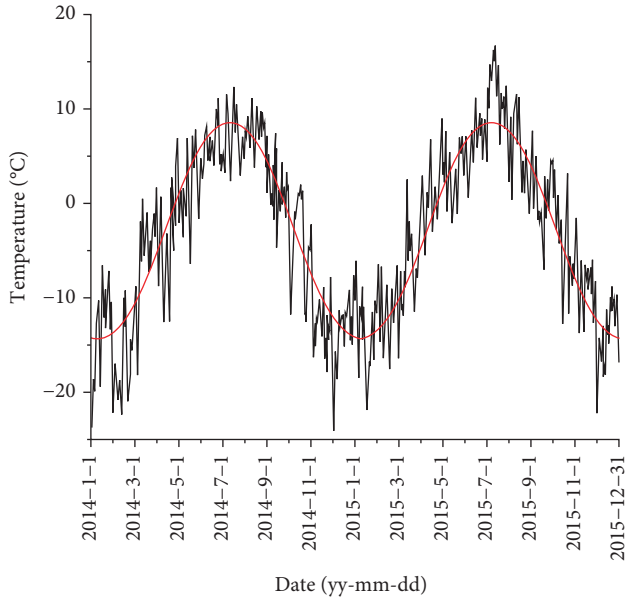

Figure 5: The temperature data of Y5854 weather station from 2014 to 2015.

$$T = 0.1 + 13\sin\left(\frac{2\pi t}{8760} - 0.56\pi\right). \quad (12)$$

5. Calculation Results and Analysis

5.1. Surface Temperature of Roadbed under Snow Cover.

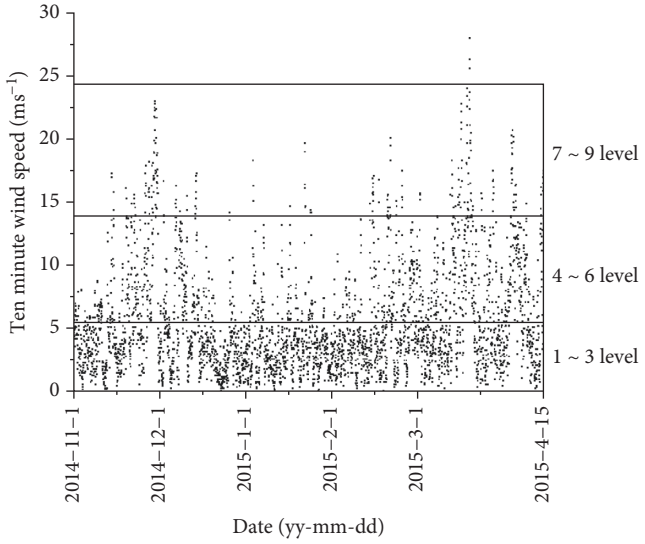

Figure 6: Ten-minute wind speed obtained by Y5854 weather station in winter from 2014 to 2015.

Figure 7 shows the temperature of the roadbed surface under different thicknesses of snow cover. The deeper the snow cover thickness on the roadbed superficial region, the smaller the variation of its surface temperature. Surface temperatures without snow cover are at their lowest around January 10. When 10 cm, 30 cm, 50 cm, and 70 cm of snow cover thicknesses, the lowest temperature occurred on February 2, 12, 17, and 27. The minimum temperature has been delayed for up to 48 days. Compared with the ground temperature with no snow cover, 70 cm snow cover

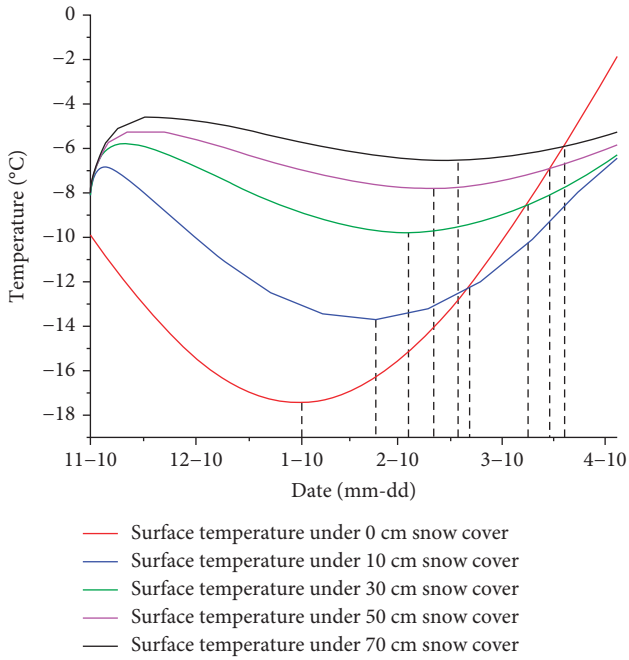

Figure 7: The surface temperature under different depths of snow cover.

thicknesses have a minimum temperature difference of 11°C. This is the same as the ground temperature and snow surface temperature results detected at five points in Changji, Xinjiang [36]. Snow cover blocks the thermal exchange between the environment and the frozen soil, forms a good thermal insulation effect on the ground, and significantly postpones the occurrence of the lowest temperature [19]. As the atmospheric temperature rises, snow cover blocks the warming effect of the atmosphere on the ground. The larger the snow cover thickness, the less the surface warming. This phenomenon will continue until the snow has completely thawed.

5.2. Temperature Field under Roadbed

5.2.1. Temperature Field of the Road Surface without Snow Cover. As shown in Figure 8, the temperature at different depths below the left and right road borders changes with time after the roadbed has been in operation for 30 years without considering the increase in the atmospheric temperature. The sunny-shady slope effect is formed due to the different orientations of the roadbed slope, resulting in different thermal exchange between the superficial region and the environment, and different amounts of radiation received by the slope. For the part-cut part-fill roadbed, the slope orientation and slope gradient of the left and right sides of the roadbed are the same, and their temperature is also the same. However, due to the upward excavation of the right-side slope, the distance from the solar radiation to the right roadbed becomes farther, resulting in the temperature field under the roadbed being seriously asymmetrical. The frozen soil temperature under the left road border at the same depth is significantly higher than that of the right road border. The left road border's 0°C isotherm (upper limit of frozen soil) is 1.3 m lower than the 0°C isotherm (upper limit of frozen soil) of the right road border. The temperature at different depths under the roadbed on October 1, the 30th year of roadbed operation, is shown in Figure 9. When there is no snow cover (0 cm), the temperature of the frozen soil at the roadbed center increases by 0.3°C compared with that of the natural slope.

5.2.2. Temperature Field of the Road Surface Covered by Snow. As shown in Figures 8(b)–8(e), the temperature of the frozen soil under the roadbed covered by snow increases more significantly than that of the road without snow cover. This accelerates the degradation of the frozen soil. The thicker the snow cover, the higher the temperature increment of the frozen soil under the roadbed. By comparing Figures 8(a) and 8(e), the snow cover significantly increases the frozen soil range under the left and right road borders thawed throughout the year. The 70 cm snow cover makes the 0°C isotherm varied with time under the left road border develop 16 cm downward. However, the 0°C isotherm under the right road border develops downward by 59 cm. The snow cover causes the temperature increment under the right road border to be significantly higher than the left road border.

Snow is a poor heat conductor. Snow cover delays the superficial temperature rise, delaying the start time of frozen soil thawing at different locations under the roadbed. Due to the thermoinsulation effect of snow cover on the road surface, the thicker the snow, the more obvious the thermal insulation effect. This results in less cold energy being stored in the roadbed in winter and a longer time needed for the thawing plate under the roadbed to disappear completely. The time for the thawing plate under the right road border to disappear completely is extended from early to late November. Therefore, the snow cover has a delayed effect on the time of thawing start and freezing completion of the activity layer under the roadbed.

As shown in Figure 9, the snow cover increases the temperature of the frozen soil under the roadbed. When the thickness of the snow cover is approximately 10 to 70 cm, the temperature of frozen soil will increase by about 0.2°C to 0.75°C. The snow cover puts the low-temperature frozen soil under the roadbed at risk of transforming into the high-temperature frozen soil. This is because the snow cover causes changes in the thermal status of the soil, which influences the temperature of the frozen soil and the activity layer under the roadbed [5]. The snow cover can isolate the cold air effect and play a heat preservation role. The greater the snow thickness, the higher the temperature of the frozen soil under the roadbed.

5.3. Frozen Soil Upper Limit for Roadbed under Snow Cover

5.3.1. Frozen Soil Upper Limit for Roadbed without Snow Cover. The changes in the frozen soil upper limit after the road border operation for about 30 years are shown in Figures 10 a and b. The frozen soil upper limit under the left

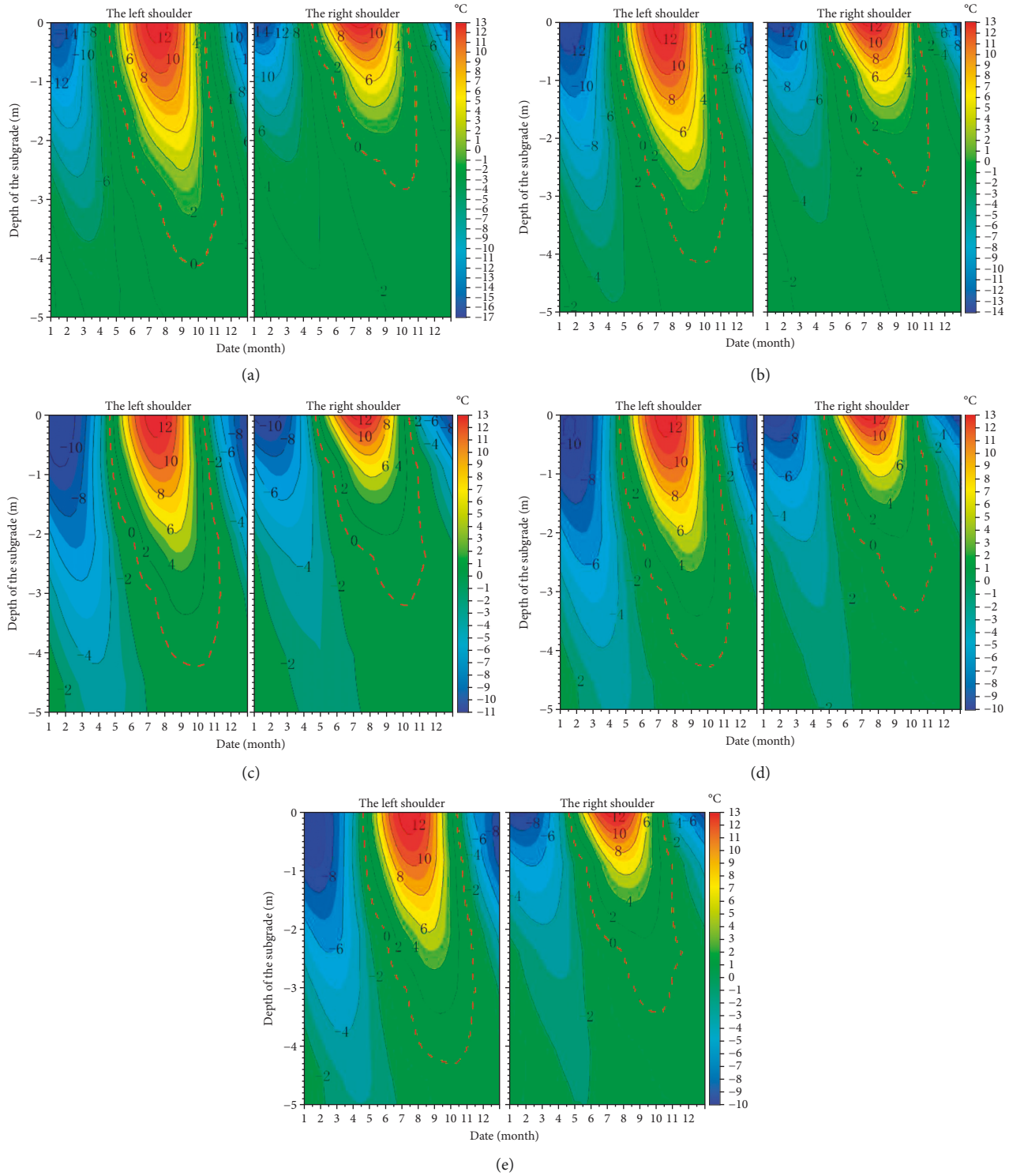

FIGURE 8: The temperature of different thicknesses of snow cover varies with time under roadbed after 30 years of operation, (a) 0 cm snow cover, (b) 10 cm snow cover, (c) 30 cm snow cover, (d) 50 cm snow cover, (e) 70 cm snow cover.

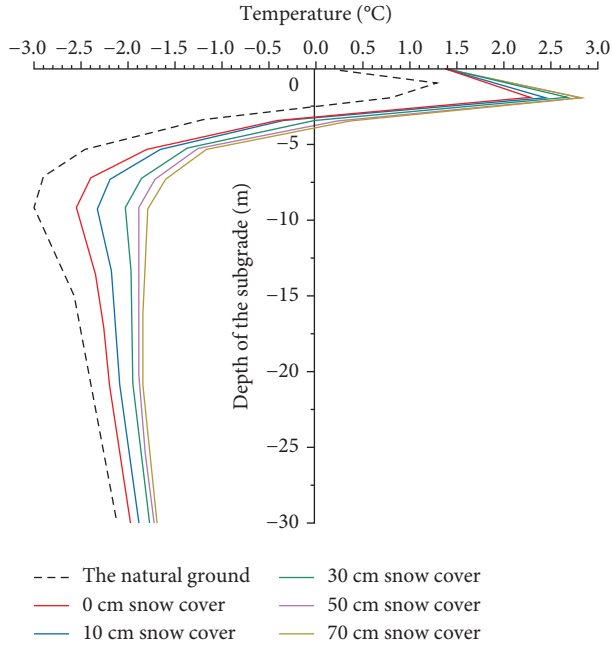

Figure 9: The temperature on October 1 of the roadbed after 30 years operation.

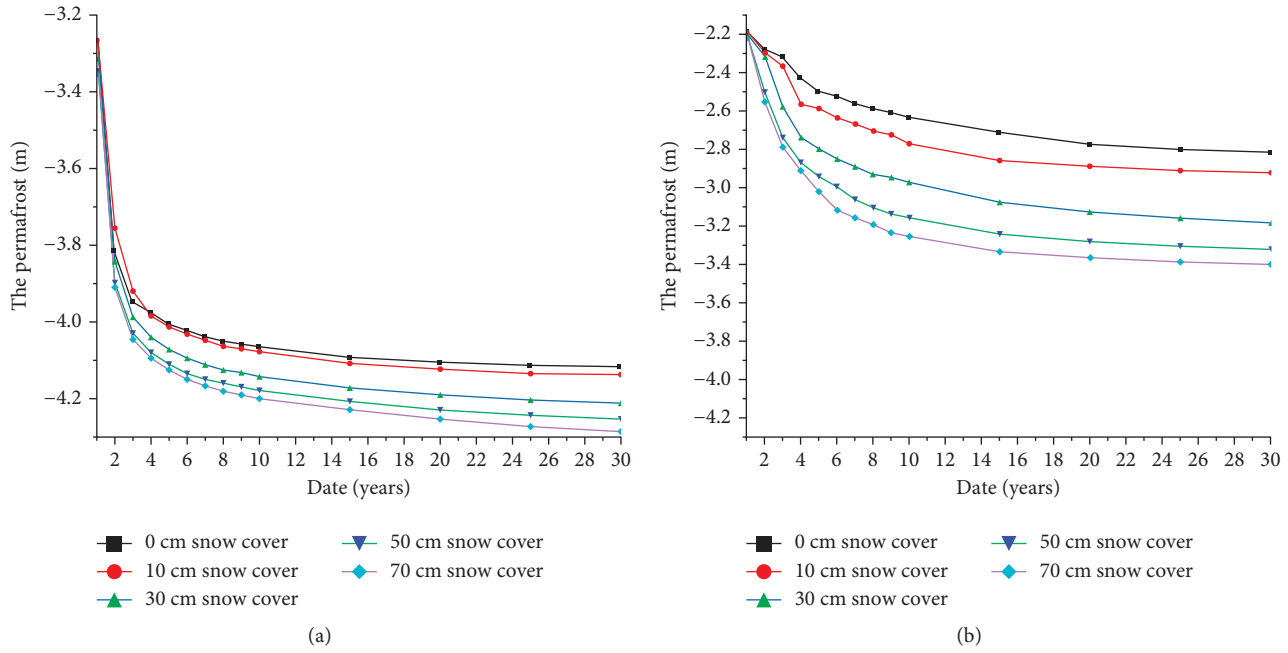

Figure 10: The frozen soil upper limit under different depths of snow cover, (a) Left road border, (b) Right road border.

road border decreased by 71 cm in the first 4 years, and its decline rate was fast. From the 4th to the 20th year, the frozen soil upper limit decreased by 14 cm, and its decline rate slowed down. After 20th years, the frozen soil upper limit under the roadbed has reached a stable state. The frozen soil upper limit under the left road border has dropped the most in the first four years.

The frozen soil upper limit under the right road border is falling more slowly than the left road border. In the first 10 years of roadbed construction, the frozen soil upper limit has been declining for a long time, dropping 53 cm. In the 10th to 20th years, it dropped 15 cm. After the 20th years, the frozen soil upper limit has also attained a relatively steady status.

Figure 11 displays the relationship between the frozen soil upper limit and the snow cover thickness under the roadbed. When there is no snow cover (0 cm) before and after the roadbed construction, the frozen soil upper limit under the roadbed is lower than the natural ground. Its influence range is within 3 m areas outside the left and right

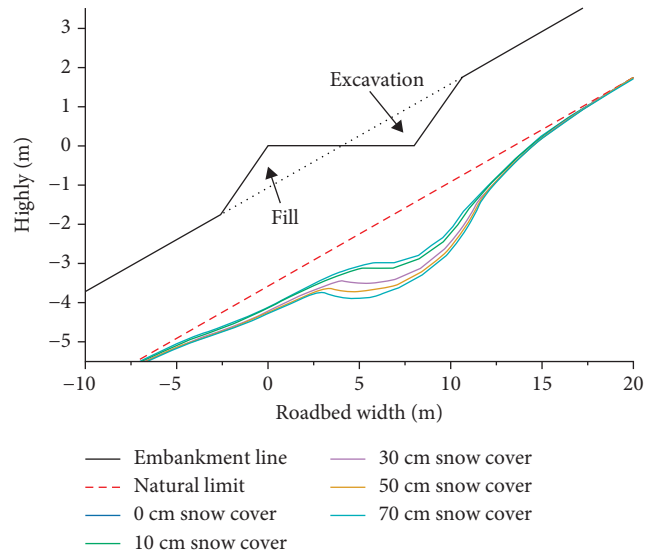

Figure 11: The frozen soil upper limit under the roadbed on October 1 after 30 years of roadbed operation.

Table 4: Frozen soil upper limit of roadbed under different thickness of snow cover.

Position (m)	0 cm snow cover	10 cm snow cover	30 cm snow cover	50 cm snow cover	70 cm snow cover
Left road border	4.12	4.14	4.21	4.25	4.28
Roadbed central line	3.21	3.27	3.44	3.70	3.87
Right road border	2.82	2.93	3.19	3.32	3.41

slope feet. The frozen soil upper limit under the roadbed is inclined to the left and right, and their difference reaches about 1.3 m, as shown in Table 4. Unlike the high roadbed built in the flat frozen soil areas, the frozen soil upper limit of the left side of the center of the roadbed is raised. Due to the steep natural slope (15°), the angle (1 : 1.5) and the roadbed side slope area are large. The filling of the roadbed does not increase the frozen soil upper limit but only restricts the downward trend of the upper limit. This can protect the frozen soil under the roadbed. While excavation on the right side of the roadbed, the degradation of frozen soil is more serious. This is also why the part-cut part-fill roadbed in cold mountain areas is prone to diseases such as uneven subsidence and thaw slumping.

5.3.2. Frozen Soil Upper Limit of Snow-Covered Roadbeds. As displayed by Figure 11, when the roadbed superficial region is covered with snow, and the frozen soil upper limit is relatively uncovered by snow, the upper limit moves down in an all-round way, and the drop on the right side of the roadbed is larger. As shown in Table 4, when the snow thickness is less than 10 cm, its impact on the frozen soil upper limit under the roadbed is small. When the snow thickness is 70 cm, the frozen soil upper limit under the left roadbed moves down by about 16 cm, and the upper limit under the right roadbed moves by 59 cm. In October, there is a thawing hollow generated under the right roadbed. With the increase in snow cover, the frozen soil lower limit is more significant. The thawing hollow develops downward and towards the centerline of the roadbed. In winter, under the roadbed covered by 70 cm thick snow, the thawing hollow spreads to the position of the roadbed centerline. The frozen soil upper limit is inclined under the roadbed, and the upper limit is shallower under the right roadbed. Under the thermal insulation effect of snow, the degradation of the frozen soil under the right roadbed is more obvious. Therefore, it should not ignore the impact of snow cover on the roadbed temperature field and frozen soil activity layer. The increase and uneven thickness of the frozen soil activity layer under the roadbed will also affect the roadbed deformation.

6. Conclusions

(1) After the part-cut part-fill roadbed is built in the cold mountain areas, due to the geometric asymmetry of the fill and cut and the slope, the temperature of the frozen soil increases, and the frozen soil also degrades. The degradation rate of frozen soil under the left road border is significantly faster than that of the right road border, and the lateral asymmetry of the temperature field is serious.

(2) Snow cover on the roadbed surface accelerates the degradation of the frozen soil, and its temperature rises significantly. The road surface has no snow cover when the snow thickness is 10 cm to 70 cm. After 30 years of roadbed operation, the temperature of frozen soil has increased by 0.2°C to 0.75°C. The low-temperature frozen soil under the roadbed has the risk of transforming into high-temperature frozen soil.

(3) The snow cover increases the thickness of the frozen soil activity layer under the roadbed, and the frozen soil upper limit decreases. The frozen soil upper limit on road borders is low on the left and high on the right, and snow cover exerts a greater influence on the frozen soil upper limit on the right road border. In October, there is a thawing hollow generated under the right roadbed. When the thickness of snow elevated, the area of the thawing hollow expanded and developed toward the center of the roadbed.

Data Availability

The data used to support the findings of the study are included within the article.

Conflicts of Interest

The authors declare that the research was conducted in the absence of any commercial or financial relationships that could be construed as potential conflicts of interest.

Acknowledgments

The project was supported by the Natural Science Foundation of Xinjiang Uygur Autonomous Region, No. 2020D01C025.

References

[1] P. J. Li, "Distribution of snow cover 0ver the high Asia," *Journal of Glaciology and Geocryology*, vol. 17, no. 04, pp. 291–298, 1995.

[2] P. J. Li, "Dynamic characteristic of snow cover in western China," *Acta Geographica Sinica*, vol. 48, no. 06, pp. 505–515, 1993.

[3] J. Q. Chou and X. H. Sun, "Preliminary study on snow cover in the tianshan mountains," *Arid Land Geography*, vol. 15, no. 03, pp. 9–21, 1992.

[4] L. E. Goodrich, "The influence of snow cover on the ground thermal regime," *Canadian Geotechnical Journal*, vol. 19, no. 04, pp. 421–432, 1982.

[5] S. B. Liu, S. Y. Zhan, L. J. Zhang et al., "Analyzing the spatial-temporal variations of snow depth in the Northeast China by means of remote sensing in consideration of frozen ground zonation," *Journal of Glaciology and Geocryology*, vol. 40, no. 02, pp. 261–269, 2018.

[6] H. Park, A. N. Fedorov, M. N. Zheleznyak et al., "Effect of snow cover on pan-Arctic permafrost thermal regimes," *Climate Dynamics*, vol. 44, no. 9-10, pp. 2873–2895, 2015.

[7] Q. Fu, R. J. Hou, Z. L. Wang, L Tianfu, and W Xianghao, "Soil thermal regime under snow cover and its response to meteorological factors," *Transactions of the Chinese Society for Agricultural Machinery*, vol. 46, no. 07, pp. 154–161, 2015.

[8] X. W. Fan, Z. J. Lin, J. Luo, L Minghao, Y Guo'an, and G Zeyong, "Long-term effects of embankment engineering behaviors on cold permafrost in high-altitude permafrost regions," *Journal of Glaciology and Geocryology*, vol. 43, no. 05, pp. 1323–1333, 2021.

[9] X. Zhang, Y. Jiang, G. Wang, Y. Cai, and T. Iura, "Three-dimensional seismic performance of mountain tunnel with imperfect interface considering P wave," *Tunnelling and Underground Space Technology*, vol. 108, 2021.

[10] H. Ma and R. J. Hu, "Effects of snow cover on thermal regime of frozen soil," *Arid Land Geography*, vol. 43, no. 04, pp. 23–27, 1995.

[11] L. Q. Hu, P. F. Wu, W. H. Zhang, and F. C. Liang, "Analyzing the effect of snow cover in spring and winter and air temperature on frozen ground depth in Xinjiang," *Journal of Glaciology and Geocryology*, vol. 36, no. 01, pp. 48–54, 2014.

[12] T. Zhang, T. E. Osterkamp, and K. Stamnes, "Effects of Climate on the Active Layer and Permafrost on the North Slope of Alaska, U.S.A," *Permafrost and Periglacial Processes*, vol. 8, no. 1, pp. 45–67, 1997.

[13] M. J. Lafrenière, E. Laurin, and S. F. Lamoureux, "The impact of snow accumulation on the active layer thermal regime in high Arctic soils," *Vadose Zone Journal*, vol. 12, no. 1, 2013.

[14] H. Wu, G.-y. Zhao, and S.-w. Ma, "Failure behavior of horseshoe-shaped tunnel in hard rock under high stress: Phenomenon and mechanisms," *Transactions of Nonferrous Metals Society of China*, vol. 32, no. 2, pp. 639–656, 2022.

[15] W. Haeberli, "Die Basis-Temperatur der winter-lichen Schneedecke als moglicher Indikator fur die Verbreitung von Permafrost in den Alpen," *Zeitschrift fur Gletscherkunde und Glazialgeologie*, vol. 9, pp. 221–227, 1973.

[16] M. Stieglitz, "The role of snow cover in the warming of arctic permafrost," *Geophysical Research Letters*, vol. 30, no. 13, pp. 54–51, 2003.

[17] P. Pogliotti, M. Guglielmin, E. Cremonese et al., "Warming permafrost and active layer variability at Cime Bianche, Western European Alps," *The Cryosphere*, vol. 9, no. 2, pp. 647–661, 2015.

[18] G. Han, Yu Zhou, R. Liu, Q. Tang, X. Wang, and L. Song, "Infuence of surface roughness on shear behaviors of rock joints under constant normal load and stifness boundary conditions," *Natural Hazards*, vol. 2, pp. 1–18, 2022.

[19] Q. Fu, R. Hou, T. Li, M. Wang, and J. Yan, "The functions of soil water and heat transfer to the environment and associated response mechanisms under different snow cover conditions," *Geoderma*, vol. 325, pp. 9–17, 2018.

[20] D. Pan, K. Hong, H. Fu, J. Zhou, and N. Zhang, "Experimental Study of the Mechanism of Grouting Colloidal Nano-Silica in Over-Broken Coal Mass," *The Quarterly Journal of Engineering Geology and Hydrogeology*, vol. 54, no. 4, pp. qjegh2020–161, 2021.

[21] D. Pan, K. Hong, H. Fu, J. Zhou, N. Zhang, and G. Lu, "Influence characteristics and mechanism of fragmental size of broken coal mass on the injection regularity of silica sol grouting," *Construction and Building Materials*, vol. 269, Article ID 121251, 2021.

[22] X. Z. Yu, F. H. Yuan, A. Z. Wang, W Jia-bing, and G De-xin, "Effects of snow cover on soil temperature in broad-leaved Korean pine forest in Changbai Mountains," *Yingyong Shengtai Xuebao*, vol. 21, no. 12, pp. 3015–3020, 2010.

[23] Z. Wen, O. Jian, Y. Daoxue, W. Xiaojun, G. Zhongqun, and Hu Kaijian, "Effect of the in situ leaching solution of ion-absorbed rare earth on the mechanical behavior of basement rock," *Journal of Rock Mechanics and Geotechnical Engineering*, 2022.

[24] G. Li, Y. Zhao, W. Zhang, and X. Xu, "Influence of snow cover on temperature field of frozen ground," *Cold Regions Science and Technology*, vol. 192, Article ID 103402, 2021.

[25] W. Q. Tao, *Numerical Heat Transfer*, Xi 'an Jiaotong University Press, Xi'an, Shaanxi, China, 2001.

[26] M. T. Van Genuchten, "A Closed-form Equation for Predicting the Hydraulic Conductivity of Unsaturated soils," *Soil Science Society of America Journal*, vol. 44, no. 5, pp. 892–898, 1980.

[27] G. S. Taylor and J. N. Luthin, "A Model for Conpled Heat and Moisture Transfer during Freezing," *Canadian Geotechnical Journal*, vol. 15, pp. 548–555, 1987.

[28] X. Z. Xu and Y. S. Deng, *Experimental Study on Water Migration in Frozen Soil*, Beijing Science Press, Beijing, China, 1991.

[29] Z. C. Yang, D. Wei, and D. Chen, "Study on soil freezing and water migration under different snow cover conditions," *Water Conservancy Science and Technology and Economy*, vol. 13, no. 06, pp. 365–367, 2007.

[30] M. Sturm, J. Holmgren, M. König, and M Kim, "The thermal conductivity of seasonal snow," *Journal of Glaciology*, vol. 143, pp. 26–41, 1997.

[31] X. Z. Xu, J. C. Wang, and L. X. Zhang, *Frozen Soil Physics*, Science Press, China, 2001.

[32] Y. Y. Wang, H. Q. Guo, and Y. S. Ye, "Numerical Analysis of Frozen Soil Temperature Field in a Short Period of Subgrade Filling in Permafrost Region," *China Railway Science*, vol. 42, no. 4, pp. 9–18, 2021.

[33] Q. B. Bai, *Determination of Boundary Layer Parameters and a Preliminary Research on Hydrothermal Stability of Subgrade in Cold Region*, Beijing Jiaotong University, China, 2016.

[34] P. X. Li, *Study on Formation Mechanism and Prevention Technology of Wind and Snow Disaster on Afuzhun Railway*, Beijing Jiaotong University, China, 2019.

[35] K. Gisnås, S. Westermann, T. V. Schuler et al., "A statistical approach to represent small-scale variability of permafrost temperatures due to snow cover," *The Cryosphere*, vol. 8, no. 6, pp. 2063–2074, 2014.

[36] X. Q. Wang, X. Y. Lu, and J. F. Wang, "Relation between Snow Surface and Ground Temperature at Different Snow Depths," *Meteorological Science and Technology*, vol. 41, no. 06, pp. 1068–1072, 2013.

[37] G. Y. Wang, H. Y. Mao, B. He, Q. B. Wu, and Y. P. Shen, "Changes in Snow Covers during 1961-2011 and Its Effects on Frozon Ground in Altay Region,Xinjiang," *Journal of Glaciology and Geocryology*, vol. 34, no. 06, pp. 1293–1300, 2012.

[38] T. Zhang, "Influence of the seasonal snow cover on the ground thermal regime: An overview: SNOW cover and ground thermal regime," *Reviews of Geophysics*, vol. 43, no. 4, 2005.

[39] M. L. Zhang, Z. Wen, K. Xue, and C. L. Zhi, "Influence of Slope Seepage on Thermal Regime of Qinghai-Tibet Highway in Permafrost Regions," *Highways*, vol. 61, no. 07, pp. 13–19, 2016.

[40] Y. B. Cao, Y. Sheng, J. C. Wu et al., "Influence of upper boundary conditions on simulated ground temperature field in permafrost regions," *Journal of Glaciology and Geocryology*, vol. 36, no. 04, pp. 802–810, 2014.